Structures of Glasses Created by Multiple Kinetic Arrests

Junguang Yu[1], Zhenxuan Chen[1], Rattavut Teerakapibal[1], Chris Benmore[2], Ranko Richert[3], Lian Yu[1,4,*]

[1] School of Pharmacy, University of Wisconsin-Madison, Madison, WI, 53705, USA

[2] X-ray Science Division, Advanced Photon Source, Argonne National Laboratory, IL, 60439, USA

[3] School of Molecular Sciences, Arizona State University, AZ, 85287, USA

[4] Department of Chemistry, University of Wisconsin-Madison, Madison, WI, 53705, USA

ABSTRACT. X-ray scattering has been used to characterize the structure of glassy itraconazole (ITZ) prepared by cooling at different rates. Faster cooling produces ITZ glasses with lower or zero smectic order, larger inter- or intralayer spacing, more sinusoidal shape of density modulation, and shorter intralayer (lateral) correlation. We characterize each glass by a set of fictive temperatures T_f that describe its smectic order and intralayer order, each corresponding to the temperature at which the chosen property is frozen in the equilibrium liquid. We find that the T_f values are significantly higher for the amplitude of the smectic density modulation and the regularity of lateral packing than for inter- or intralayer spacing. This indicates that the different aspects of structure are frozen on two different timescales. These two timescales correspond to the two relaxation modes observed by dielectric spectroscopy: the faster α mode is frozen at a lower temperature and correlates with the freezing of inter- and intralayer spacings; the slower δ mode is frozen at a higher temperature and correlates with the freezing of smectic order. Our finding suggests a way to selectively control structural features in glasses.

INTRODUCTION

The structure of glasses is often considered boring – it is whatever the precursor liquid structure is, chaotic and hard to describe. Recent work, however, has shown a glass structure can be highly ordered, with order parameters bordering on values for crystals.[1] These interesting glasses are prepared by vapor deposition[2] and by cooling liquid crystals (LCs) that have structural order in the fluid state.[3-5] The long-range order is potentially useful for optimizing charge transfer and light emission in optoelectronic devices[6] and offers an possibility to characterize structural features in glasses.

LCs are known for their ability to rapidly organize in the fluid state in response to temperature and external fields.[7] This has led to the notion that thermotropic LC transitions are thermodynamically controlled and cannot be circumvented. Recent work, however, has shown that LC transitions can be avoided partially or completely by cooling at moderate rates, leading to glass structures in which LC order is tunable by cooling rate.[3-5] Given that LCs can have multiple relaxation modes,[8-10] further inquiries were made to determine whether the freezing of LC order is associated with the kinetic arrest of a given relaxation mode. For two LCs composed of rod-like molecules, the freezing of the smectic order has been associated with the kinetic arrest of the end-over-end rotation;[3, 4] for a LC composed of discotic molecules, the freezing of the columnar order has been associated with the kinetic arrest of disc tumbling.[5]

The structure of a glass has many aspects. While the previous work focused on the smectic or columnar order, many other features may play an important role in the functions of glassy materials. Take a columnar LC for example. Besides the perfection of columns, the quality of $\pi-\pi$ stacking is expected to influence the efficiency of charge transfer.[11] For a smectic structure, it is of interest to know not only the interlayer order but also the intralayer order. More importantly, given the multiple relaxation modes in a LC system, it is of interest to learn whether different aspects of structure are frozen at different temperatures.

In this study, we perform an extensive characterization of the glass structure of itraconazole (ITZ, Scheme 1), a rod-like LC mesogen, prepared at different cooling rates. We utilize X-ray scattering to investigate several structural attributes of each glass prepared,[12] including the amplitude, shape and period of the smectic density modulation and the spacing and correlation length of the intralayer (lateral) order. As a point of reference, we investigate an analogue of ITZ, Posaconazole (POS, Scheme 1), which has a similar structure but does not form LCs. We find that ITZ glasses prepared by different cooling rates have very different structures with respect to smectic and lateral packing. By comparison with the structure of the equilibrium liquid, we find the different structural features in a glass are frozen at very different temperatures; that is, the glass has different fictive temperatures with respect to the different structural attributes. The regularity of smectic layers and the intralayer correlation length are frozen at a higher temperature than the

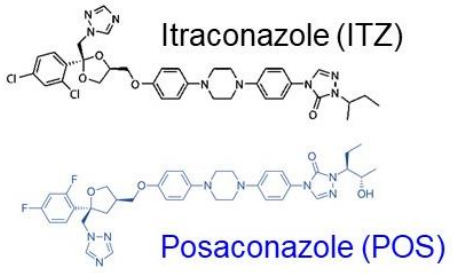

Scheme 1. Structures of itraconazole (ITZ) and posaconazole (POS).

interlayer and intralayer spacing. The former corresponds to the kinetic arrest of the slow relaxation mode δ (end-over-end rotation) and the latter to that of the fast relaxation mode α (rotation about the long axis). Our finding provides guidance for the rational design for the structure of glasses.

EXPERIMENTAL METHODS

Materials and Sample Preparation. Itraconazole (ITZ, 98% pure) was purchased from Alfa Aesar (Ward Hill, MA) and posaconazole (POS, 99% pure) from BioChemPartner (Shanghai). Both were used as received. Crystalline ITZ or POS powder was filled into a capillary tube (Charles-supper, MA, 1.5 mm OD, 10 μm wall thickness) and the tube was flame sealed. A glass sample was prepared by melting the crystals and cooling the melt at different rates. Cooling rates lower than 1 K/s were obtained using the DSC sample cell. Cooling rates of 1 K/s and 2 K/s were obtained using a Linkam microscope hot/cold stage. Cooling rates of 20 K/s and 120 K/s were obtained by plunging a sample tube preheated to 470 K into an ice-water bath or a liquid nitrogen bath, respectively. Rate of cooling by bath was measured by performing the same cooling procedure with a thermocouple coated with a layer of epoxy 1.5 mm thick.

X-ray Scattering. Simultaneous SAXS (Small Angle X-ray Scattering) and WAXS (Wide Angle X-ray Scattering) measurements were performed using a synchrotron source at the 6-ID-D beam line in the Advanced Photo Source, Argonne National Lab. The experiment setup is shown in Scheme 2.[12] Temperature was controlled by an Oxford Cryo-system 700. Two amorphous silicon area detectors were placed at different sample-to-detector distance with each detector covering half of the azimuthal angle. Each two-dimensional image was integrated using the software FIT2D[13] to yield a one-dimensional intensity vs q plot, where $q = 4\pi\sin\theta/\lambda$. Diffraction angles were calibrated using silver behenate for SAXS and CeO_2 for WAXS. The corrected intensity of coherent scattering intensity $I(q)$ was normalized to obtain the atom-averaged X-ray structure factor:[14]

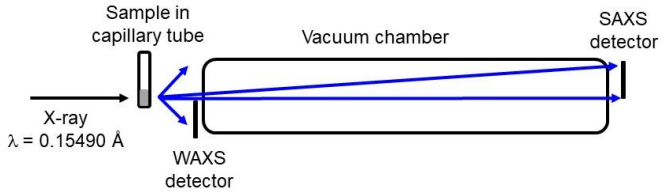

Scheme 2. Experimental setup for simultaneous synchrotron scattering of SAXS and WAXS of ITZ glasses at 300 K.

$$S(q) = 1 + \frac{I(q) - \langle f^2(q) \rangle}{\langle f(q) \rangle^2} \qquad (1)$$

where $\langle f^2(q) \rangle$ is the atom-averaged self-scattering power and $\langle f(q) \rangle^2$ is the atom-averaged scattering power of one molecule. The differential PDF, $D(r)$, was obtained by a Fourier sine transform of the function

$$F(q) = q(S(q) - 1); D(r) = \frac{2}{\pi}\int_0^{q_{max}} F(q)\ \sin(qr)\, dq$$

where q_{max} is the upper bound for usable $S(q)$ data.

X-ray scattering was also performed using the same sample with a laboratory a Cu Kα source. A Bruker D8 Discover Diffractometer with an Instec mK2000 heater was used to measure the q range 0.1−1 Å^{-1}; a Bruker D8 Venture Photon III four-circle diffractometer with an Oxford 700 Cryostream temperature controller was used for q = 0.35−2.8 Å^{-1}. Diffraction angles were calibrated with silver behenate or other crystals measured under the same conditions. Two-dimensional images were integrated using the software Datasqueeze[15] or DIFFRAC.EVA.

Differential Scanning Calorimetry (DSC). DSC was performed with a TA Q2000 Differential Scanning Calorimeter. Each sample (3−5 mg) was placed in a crimped aluminum pan. A liquid sample of ITZ was cooled at 1−20 K/min and heated at 10 K/min to study the cooling rate effect on the glass fictive temperature T_f.

RESULTS

Structural Characterization by X-ray Scattering: Smectic and Lateral Packing. Figure 1 shows the structure factors $S(q)$ of two ITZ glasses prepared by cooling at different rates: 0.08 K/s and 20 K/s, illustrating the range of structures obtainable. Both glasses were measured at 300 K using a synchrotron X-ray source. The structure factors of the two glasses are identical for q > 5 Å^{-1}. In this region scattering is dominated by the intramolecular atomic correlations and our results indicate the two glasses have the same intramolecular structure, as expected. The main difference between the two glasses is seen at low q. The slow-cooled glass shows sharp peaks at q_1 = 0.2 Å^{-1} and q_2 = 0.4 Å^{-1}, whereas the fast-cooled glass does not.[3] These peaks are associated with the presence of smectic layers. The spacing between the layers is given by $2\pi/q_1$ = 30 Å, about the length of the ITZ molecule. The q_2 peak corresponds to the second-order diffraction of the layers. The broad peak at q_L = 1.35 Å^{-1} is associated with the lateral packing of the rod-like molecule with a spacing of ~5 Å. This peak is narrower for the slow-cooled glass than for the fast-cooled glass, indicating cooling rate not only affects smectic packing, but also lateral packing. Along with increased smectic order, the lateral packing becomes more regular.

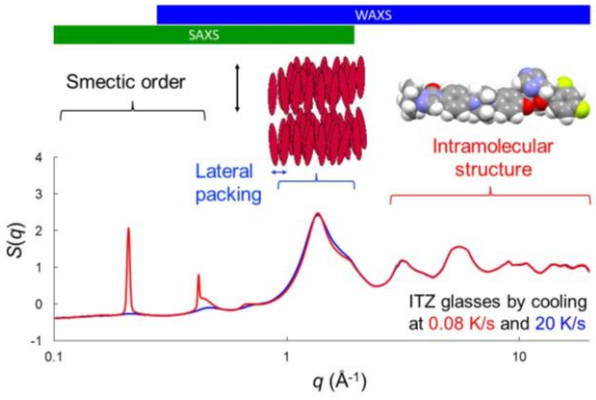

Figure 1. Structure factors of ITZ glasses at 300 K prepared by cooling at 0.08 K/s (red) and 20 K/s (blue).

Figure 2 shows the fitting of the key structural features. The q_1 peak (Figure 2a) is fitted with two Gaussians. The broader Gaussian arises from the excluded volume effect[16] and the sharper

Gaussian (area A_1) is used as a measure of the smectic order. The q_2 peak (Figure 2b) is fitted as a sum of two Gaussians and a linear baseline. The broader component at 0.44 Å^{-1} is again attributed to the excluded volume effect and the sharp component is associated with the smectic structure. The presence of q_2 peak indicates the smectic density wave is not purely sinusoidal.[16, 17]

The feature near q_L (Figure 2c) has a main peak and a shoulder to the right. This main peak is fitted as a Lorentzian:

$$S(q) = \frac{2A}{\pi}\frac{w}{4(q-q_L)^2+w^2} \qquad (2)$$

where A is peak area, q_L is peak position, and w is peak width (full width at half maximum, FWHM). The shoulder on the right is fitted with the same function. The Fourier sine transform of eq. 2 is an exponentially damped sine wave in real space whose wavelength is $2\pi/q_L$ and the correlation length $\xi = 2/w$ (ξ is the distance by which the density wave amplitude decays by $1/e$). To isolate the q_L peak, the shoulder to the right is also fitted with the function in eq. 2.

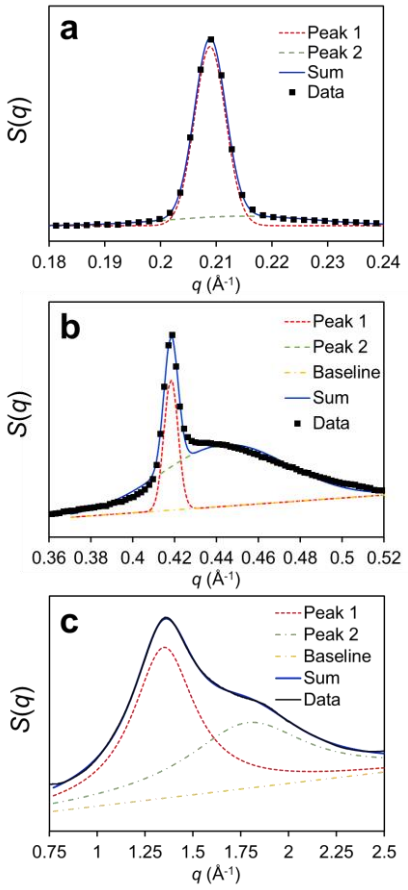

Figure 2. Fitting of key scattering peaks. The q_1 peak (a) and the q_2 peak (b) are associated with smectic order. The q_L peak (c) is associated with intralayer (lateral) packing.

Smectic and Lateral-Packing Order in the Equilibrium Liquid. Before investigating the cooling rate effects on the glass structure, we first determine the temperature dependence of the selected structural features *in the equilibrium liquid.* This information is needed later for calculating fictive temperatures. Figure 3 shows the temperature dependence of the areas (A_1 and A_2) and the positions (q_1 and q_2) of the smectic-scattering peaks. Results are shown near and above the DSC T_g (328 K), ensuring measurement of the equilibrium liquid. The data were collected by accessing the temperature region both by heating a glass (open symbols) and cooling an isotropic liquid (solid symbols); the agreement of the cooling and heating data points indicates establishment of equilibrium. Benmore et al have reported the A_1 and q_1 results[12] and we include them in Figure 3 and find excellent agreement with our results.

Figure 3a shows the peak positions q_1 and q_2 as functions of temperature. Our data indicate $q_2/q_1 = 1.999 \pm 0.003$, very close to the theoretical value of 2. The spacing between smectic layers is given by $L = 2\pi/q_1 = 4\pi/q_2$ and the calculated values are shown using the right y axis. L is approximately 3.0 nm. During cooling, L decreases, and its temperature slope yields a thermal expansion coefficient (TEC) $\alpha_1 = 932 \pm 20$ ppm/K. Notice that this is a one-dimensional TEC (along the normal of the smectic layers) and is already larger than the TEC for volumetric

expansion of typical molecular liquids (e.g., volumetric TEC = 750 ppm for *o*-terphenyl at T_m[18]). This anomalously large α_1 appears to support a S_{Ad} structure in which the degree of interdigitation varies with temperature.[19]

Figure 3b shows that with cooling, the areas of two smectic scattering peaks, A_1 and A_2, increase. This is an expected result for LCs. With cooling below the transition temperature, smectic order become more perfect, leading to stronger scattering. A_1 is directly related to the amplitude of density modulation[16] and its temperature dependence is well described by a power law[4, 20]:

$$A_1 = A_{10}\,[(T_{Sm/N} - T)/T_{Sm/N}]^x \qquad (3)$$

where A_{10} is a constant, $T_{Sm/N}$ = 347 K is the smectic-nematic transition temperature, and x is a constant between 0 and 1. Fitting the A_1 data to eq. 3 (curve in Figure 3b), we obtain x = 0.65, close to the previous value x = 0.67 based on fewer data points.[3]

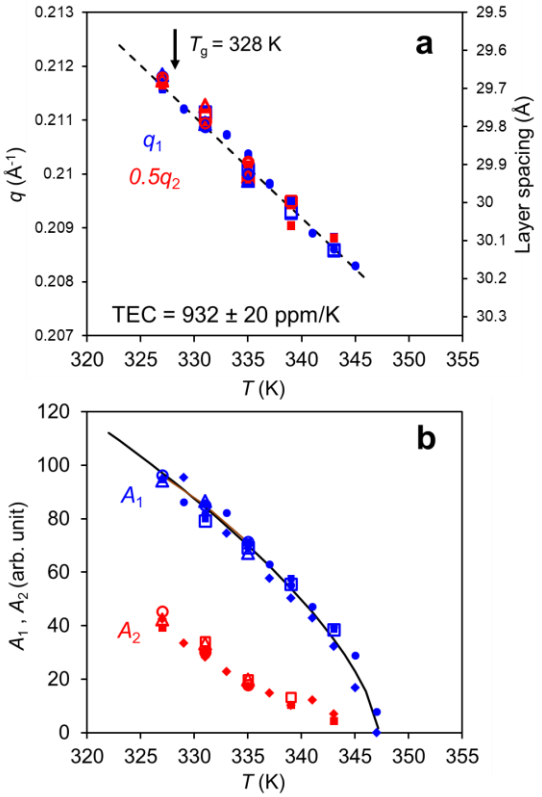

Figure 3. Temperature dependence of (a) the positions q_1 and q_2 and (b) the areas A_1 and A_2 of the smectic scattering peaks in the equilibrium state. The data were collected by accessing the temperature region by heating a glass (open symbols) and cooling an isotropic state (solid symbols). Blue and red symbols correspond to the q_1 and q_2 peaks. We observe $q_2 = 2q_1$, as expected. q_1 and q_2 have linear temperature dependence with the TEC value indicated. The black curve is a power-law fitting of the A_1 data (eq. 3). Results from Ref. 12 (solid blue circles) are in agreement with those from this work.

Figure 3b shows that the area of the q_2 peak, A_2, has a different temperature dependence from A_1. The presence of the q_2 peak means that the density modulation of the smectic layers is not perfectly sinusoidal. We find that with cooling below $T_{Sm/N}$, the ratio A_2/A_1 increases, from 0.2 to 0.4. This indicates that the deviation from sinusoidal density wave becomes greater with cooling. These observations also appear to support a S_{Ad} structure where the degree of interdigitation varies with temperature. For a simple S_A structure, one might expect a density modulation that is weakly dependent on temperature and a A_2/A_1 ratio that is nearly constant.

To fully characterize the smectic structure, it is of interest to determine the widths of the q_1 and q_2 peaks and in turn, the persistence length of density modulation. While our fitting yields these values, the peak width is mostly from the instrument resolution. Our fitting yields peak widths on the order of 0.0066 Å^{-1}whereas the instrument resolution is 0.0057 Å^{-1}. Thus we do not pursue this investigation here.

Figure 4 shows the temperature evolution of the lateral-packing peak q_L in the equilibrium liquid. For reference, results are also shown for the non-LC-forming molecule, POS. As in Figure 3, data were collected above the DSC T_g to facilitate equilibration and the temperature region was accessed by both heating a glass or cooling an isotropic liquid to demonstrate the attainment of equilibrium.

Figure 4a shows that upon cooling, q_L increases. This means the lateral spacing between molecules, given by $2\pi/q_L$, decreases with cooling. Notice that ITZ and POS show very similar contraction on cooling, with TEC α_L = 598 ± 10 ppm /K for ITZ and α_L = 605 ± 10 ppm /K for POS. This is noteworthy since in the temperature range studied, ITZ undergoes two LC transitions at $T_{Sm/N}$ and $T_{N/I}$, whereas POS shows no LC transitions, but this difference leaves little impression on this aspect of structure. In terms of lateral packing, the ITZ structure evolves with temperature just like the POS structure. It is also noteworthy that the α_L is a factor of 1.6 smaller than α_1. This large difference also suggests α_1 is irregular and possibly a result of temperature-dependent interdigitated structure.

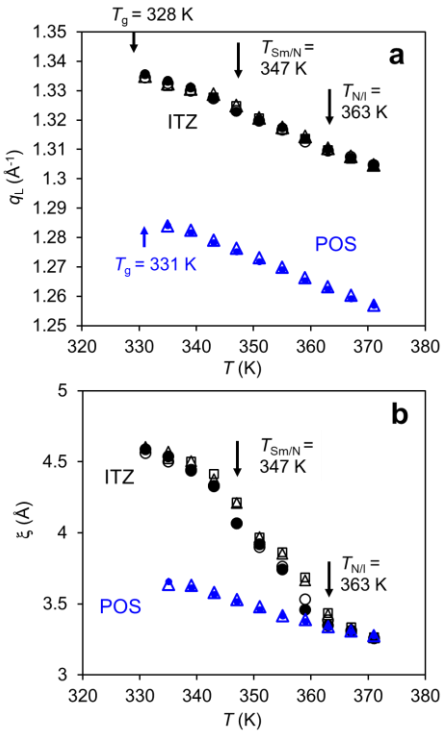

Figure 4. Temperature dependence of (a) the position q_L and (b) the correlation length ξ in the equilibrium state. The data were collected by accessing the temperature region by heating a glass (open symbols) and cooling an isotropic state (solid symbols). Data are also shown for the non-LC-forming POS as a reference.

Figure 4b shows correlation length ξ for the lateral packing of ITZ and POS in the equilibrium liquid. The ξ value is calculated from the width of the lateral-packing peak q_L. Earlier in the investigation of smectic order, we made no attempt to calculate the peak width because the observed peak width came mostly from the instrumental width. The situation is different for the lateral-packing peak since the instrument resolution, estimated to be 0.026 Å^{-1} (Figure S1), is only 5 % of the observed q_L peak width. Applying correction for instrument resolution to our data[21] resulted in no significant change of the scattering pattern (Figure S2). Thus the as-observed peak width accurately represents the intrinsic lateral correlation length. Our data show that the ξ value of POS increases linearly with cooling. This behavior is known for simple liquids; for example, ξ increases exponentially with packing fraction for densely packed spheres.[22] In comparison to POS, the ξ value of ITZ increases more rapidly with cooling. This indicates that the transition to LC phases significantly increases the regularity of lateral packing. For ITZ, the increase of ξ with cooling is not linear and appears to show jumps at the LC transition temperatures $T_{N/I}$ = 363 K and $T_{Sm/N}$ = 347 K. This further supports the view that LC ordering leads to lateral ordering.

Cooling Rate Effects on Smectic and Lateral-Packing Order. Previous work has shown that cooling rate has a significant effect on the smectic order (A_1) in the ITZ glass. We now show that the same holds for other aspects of structure but interestingly, they are affected differently by cooling rate. Figure 5 shows the cooling rate effects on the structural features of the smectic layers. ITZ glasses prepared at different cooling rates were measured at 298 K, well below T_g. Figure 5a shows that faster cooling leads to lower q_1 and q_2 values, indicating larger spacing between smectic layers. This means faster cooling freezes the system at a larger layer spacing. Figure 5b shows that faster cooling leads to lower (even zero) A_1 and A_2 values. This means smectic order is significantly degraded (ultimately erased) by fast cooling. Figure 5c shows that faster cooling leads to lower A_2/A_1 ratio (more sinusoidal density modulation).

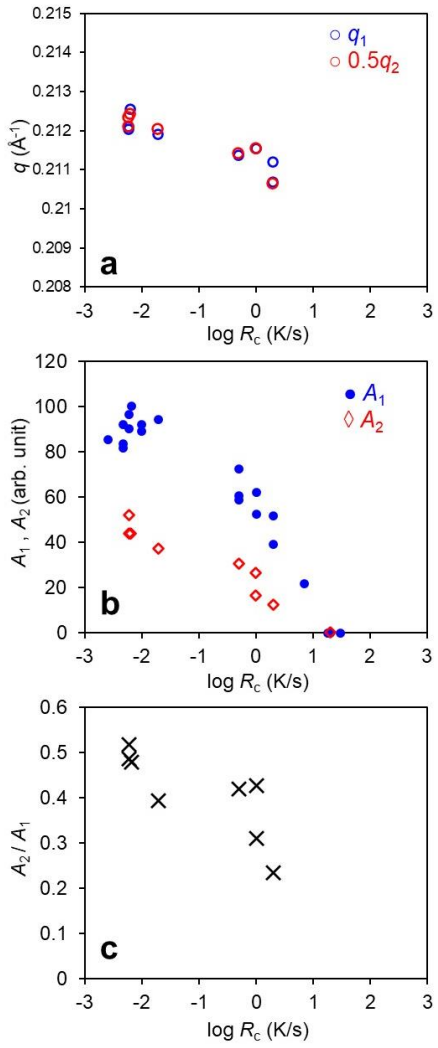

Figure 5. Cooling rate effects on (a) the areas and (b) the positions q_1 and q_2 of two smectic peaks A_1 and A_2 and (c) A_2/A_1. All glasses were measured at 298 K well below T_g. Faster cooling produces ITZ glasses with smaller A_1, A_2, A_2/A_1 and lower q_1, q_2 (larger layer spacing).

Figure 6 shows cooling rate effects on the structural features associated with the lateral packing. We see from Figure 6a that faster cooling decreases the q_L value (increases the lateral spacing). The effect is sizable, on the order of 1 %. Interestingly, the cooling rate effect on ITZ is similar to that on POS. Figure 6b shows the effect of cooling rate on the lateral correlation length. Faster cooling leads to glasses with

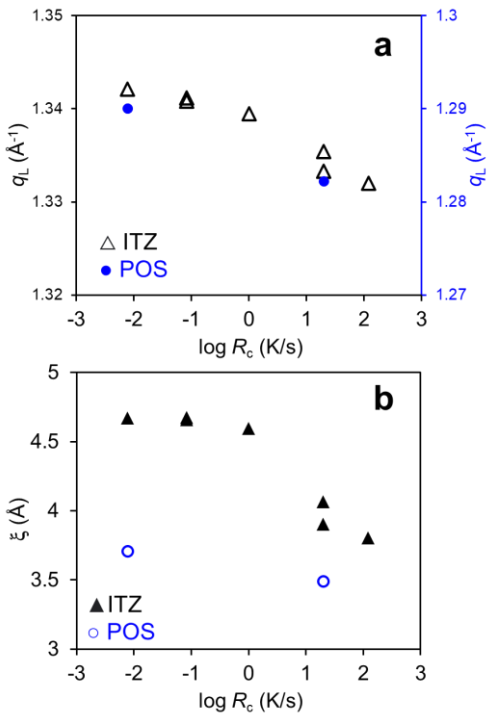

Figure 6. (a) Cooling rate effects on (a) the position q_L and (b) correlation length ξ of the lateral-packing peak. Faster cooling produces ITZ glasses with lower q_L (larger lateral spacing) and more chaotic packing.

smaller ξ values (more chaotic packing). Note that in terms of this structural attribute, cooling rate affects ITZ more strongly than it does POS: slow cooling maintains high regularity of lateral packing in ITZ, fast cooling destroys this order. In contrast, the correlation length is relatively short regardless of cooling rate.

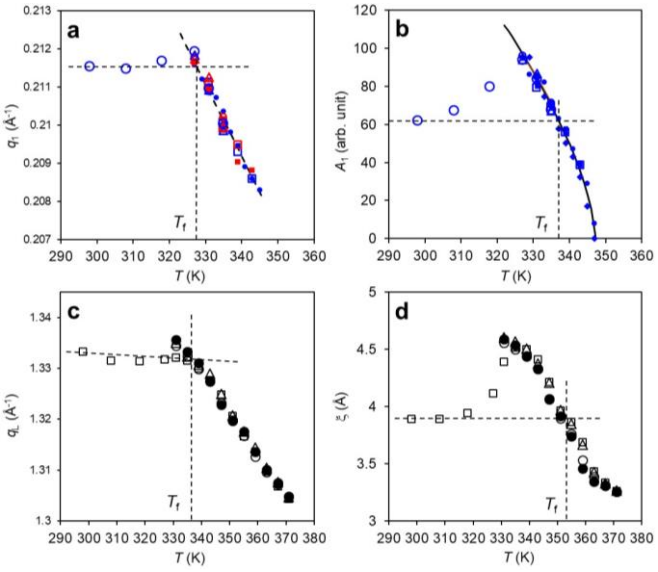

Figure 7. Measurement of the fictive temperature by heating a glass while following a chosen structural feature and comparison with the behavior of the equilibrium liquid. The structural feature of interest is (a) q_1, (b) A_1, (c) q_L, and (d) ξ. Results of (a) and (b) are from the same glass prepared by cooling at 1 K/s. Results of (c) and (d) are from the same glass prepared by cooling at 20 K/s.

Having described the range of structures obtainable in glasses prepared by cooling at different rates, we now consider their fictive temperatures; that is, the temperature of the equilibrium liquid that has the same structure according to a chosen metric as a glass of interest. A commonly used fictive temperature is defined with respect to enthalpy, $T_{f\,H}$.[23] A glass with a fictive temperature of $T_{f\,H}$ would have the structure of the equilibrium liquid at the same temperature if it is heated without structural change other than normal thermal expansion. In like manner, fictive temperatures can be defined for the structural features studied in this work. In Figure 7, we show how T_f is obtained for a feature of interest by heating a glass and comparison with the equilibrium liquid. Figure 7a and Figure 7b illustrate the determination of q_1 and A_1 in the same glass prepared by cooling at 1 K/s. It is clear that T_f values are significantly different in the same structural order. Figure 7c and Figure 7d illustrate determination of q_L and ξ in the same glass prepared by cooling at 20 K/s. Again, two significantly different T_f values are observed, indicating different aspects of structure are frozen on two different timescales.

Figure 8 shows the fictive temperatures of the glasses prepared at different cooling rates. The features used for characterizing structure include: q_1, q_2, A_1, q_L, and ξ. In addition, the common measure for fictive temperature, enthalpy H, is also used. It is noteworthy that the T_f values fall into two groups. At each cooling rate, the glass prepared has high T_f values for some structural features (A_1 and ξ) while low T_f values for others (q_1, q_2, q_L, and H). That is, some aspects of

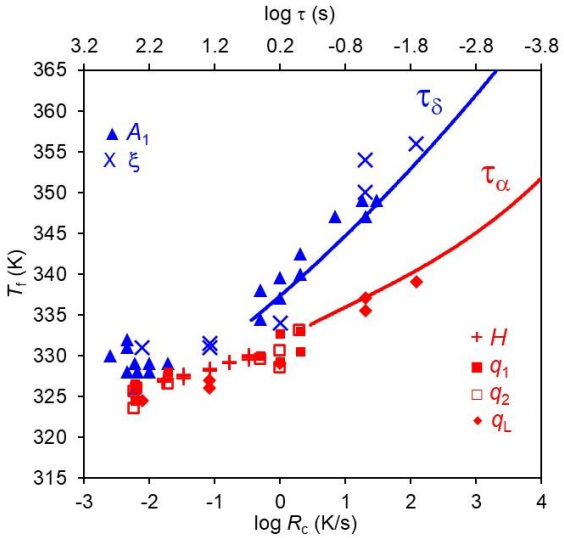

Figure 8. Cooling rate effects on T_f of each structural feature in this study, together with T_f for enthalpy. Two groups of T_f are observed, suggesting two timescales are involved in cooling rate effects.

structure are frozen at a higher temperature than others. The features frozen at a higher temperature include smectic order (A_1) and regularity of lateral packing (ξ). These correspond to structural order that requires a large number of molecules to build and presumably their cooperative rearrangement. The features frozen at a lower temperature include enthalpy and the spacings between molecules captured by q_1, q_2, and q_L. This seems sensible since molecular spacings are easily adjusted through nearest-neighbor reorganization, without cooperative rearrangements. That the enthalpy T_f falls in the same group can be justified by the fact that enthalpy is determined by the nearest-neighbor interactions.

In Figure 8 is also plotted the two relaxation timescales of ITZ observed by dielectric spectroscopy (DS).[8] The slower mode (δ) is assigned to the end-over-end rotation of the rod-like molecule, while the faster mode (α) is associated with rotation about the long axis and precession of the long axis about the electric field vector.[9] These timescales are plotted in Figure 8 using the relation

$$\tau R_c = C \quad (4)$$

where C = 1.5 is obtained by the best fit with the T_f vs R_c data.[24] The physical meaning of eq. 4 is that for a system with a single relaxation time τ, kinetic arrest is expected to occur when the cooling rate is C/τ. This value of C is slightly different from C = 0.4 determined by comparison with the T_g onset during cooling (not T_f).[3]

Figure 8 shows that the two T_f values are approximately given by the condition (eq. 4) under which the α and δ relaxation modes undergo kinetic arrest. Smectic order and lateral-packing order are frozen when the δ mode undergoes kinetic arrest; enthalpy and molecular spacings are frozen when the α mode undergoes kinetic arrest. Previous work has reached the conclusion that smectic order A_1 is controlled by the end-over-end rotation.[3, 4] Here we expand that conclusion to include the regularity of lateral packing. Furthermore we show that the other measures of structure are frozen at a much lower temperature, the T_g of the α relaxation mode.

DISCUSSION

This work has characterized the structural evolution in the equilibrium liquid state of ITZ (Figures 3 and 4) and the cooling rate effect on the structure of ITZ glasses (Figures 5 and 6). We find that the apparent thermal expansion coefficient for the smectic layer spacing is significantly larger than that for the lateral structure. An ITZ glass prepared at a given cooling rate is characterized by two fictive temperatures (Figure 8), the higher one for the smectic order and the regularity of lateral packing and the lower one for enthalpy, smectic layer spacing, and lateral spacing.

Anisotropic Thermal Expansion of ITZ and Possible Existence of Interdigitation

According to the traditional view, a smectic LC has long-range, crystal-like order in the direction perpendicular to the layers, while molecular packing within the layer is random and liquid-like.

This view is consistent with the sharp smectic scattering peak q_1 and the broad lateral scattering peak q_L. Following this view, one might expect smaller thermal expansion of the smectic layer spacing relative to the lateral spacing, $\alpha_1 < \alpha_L$. This expectation appears consistent with some LCs.[25] For ITZ, however, we observe the opposite effect: $\alpha_1 =$ 932 ± 20 ppm/K and $\alpha_L =$ 598 ± 10 ppm/K. Furthermore, the α_1 value is surprisingly large relative to the typical volumetric expansion of molecular liquids. For example, α_V = 750 ppm/K for *o*-terphenyl, implying a linear expansion coefficient of 250 ppm/K, which is significantly smaller than α_1. Though ITZ's α_L value is also rather large in this comparison, it is similar to the value for POS (605 ± 10 ppm /K) and thus is unrelated to LC order.

The large α_1 value of ITZ indicates a rapid contraction of the smectic layer spacing with cooling. This is surprising given that IR measurements indicate that the molecules become more parallel to each other with cooling.[8] For a simple smectic structure (S_A) in which the layer spacing is the monolayer thickness, one would expect an increase of layer spacing, not a decrease. We speculate that the large α_1 value of ITZ is a result of layer interdigitation. If the layers interpenetrate, the apparent layer spacing is a function of the monolayer thickness and the degree of interdigitation. In this model, the large α_1 value stems from a change of the degree of interdigitation with temperature. Interdigitation has been observed for many LCs accounting for the larger layer spacing L than the molecular length l.[19,26,27] For a series of LCs with $L/l > 1.7$, Madhusudana et al. observed rapid contraction of layer spacing with cooling with $\alpha_1 >$1500 ppm/K[19] and attributed the effect to a change of interdigitation with temperature. For ITZ, l = 25 Å based on its crystal structure (two polymorphs with root name TEHZIP in the CSD) and its monolayer thickness is $l \cos \theta$, where is the average angle of the molecule relative to the smectic-layer normal. From $S = \langle 3/2 \cos^2\theta - 1/2 \rangle = 0.7$,[8] we obtain $\theta = 26°$ and $l \cos \theta = 22$ Å for the monolayer thickness. This thickness is much small than the apparent layer thickness from scattering L = 30 Å, implying a need for interdigitation in forming smectic layers. We speculate that cooling leads to a greater degree of interdigitation and to a large α_1 value.

Figure 9 shows a possible model for the smectic layer. This layer contains two sublayers of molecules offset from each other so that the total layer thickness is L = 30 Å. The angle between the molecule's long axis and the LC director is 26°, be consistent with S = 0.7.[8] The molecules are arranged anti-parallel to agree with the crystal structure. The offset between the molecules is chosen to be 4 Å, the same as that between adjacent molecules in crystals. This structure yields a diffraction pattern in close agreement with the observed pattern (Figure 9b). The proposed model is reasonably stable as changing the offset would change the relative intensities of the two diffraction peaks to deviate from the experimental result. We find that A_2/A_1 is very sensitive

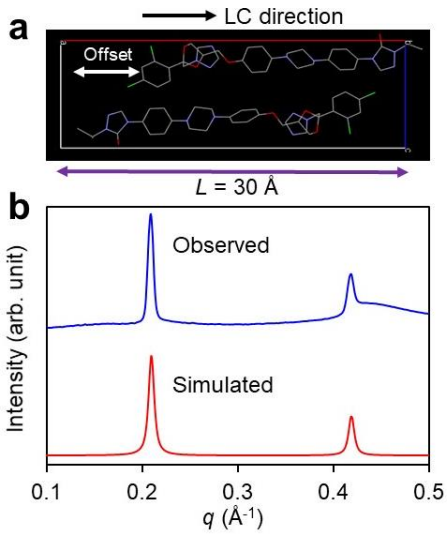

Figure 9. (a) A molecular model for offset ITZ molecules comprising a smectic layer. (b) Simulated pattern of this model is consistent with the observed X-ray diffraction pattern for a glass prepared by cooling at 0.08 K/s.

to the degree of interdigitation (molecular offset). By changing the offset, it is possible to reproduce the diffraction patterns of glasses prepared at other cooling rates.

Structures of Glasses Created by Multiple Kinetic Arrest. A key result of this work is that it is possible to create glasses in which structural features are frozen at very different temperatures. Stated in terms of fictive temperatures, the same glass can have multiple fictive temperatures with respect to different structural features. For an ITZ glass prepared by cooling at a given rate, the smectic order and the lateral-packing regularity correspond to a higher-temperature liquid than its enthalpy and inter- and intralayer spacing. For a glass quenched at 100 K/s, the two fictive temperatures above differ by 20 K. This is the reason why some aspects of structure can be altered by cooling rate to a greater extent than others. The ability to selectively alter some aspects of structure is intrinsic to glass formation as a system in equilibrium, by definition, is characterized by a single temperature.

The fact that smectic order and lateral correlation length are frozen at the same temperature argues these two aspects of structure are coupled. The increase of smectic order is accompanied by the more parallel alignment of the rod-like molecules (i.e., increase of orientational order).[8] It makes sense that this leads to more regular packing in the lateral direction. This viewpoint is supported by the simultaneous rise of smectic order (Figure 3b) and lateral-packing order (Figure 4b) as the equilibrium liquid enters the smectic phase. The smectic order emerges from zero, while the lateral-packing order increases relative to the non-LC system POS as reference. The lateral correlation length of POS increases linearly with cooling, while the value of ITZ shows jumps at the LC transition temperatures, supporting the simultaneous development of smectic and lateral-packing order. We note that this conclusion is somewhat contradictory to the traditional view that a smectic LC is ordered only with respect to the repeating layers and disordered within the layers. We find that interlayer order and intralayer order grow together.

In contrast to smectic and lateral order, this work has shown that the glass structure gauged by enthalpy, smectic layer spacing, and lateral spacing are frozen together at a lower temperature. This result echoes the previous report that for a discotic LC, columnar order is frozen at a higher temperature than inter-columnar spacing.[5] These results are sensible since the distance between molecules is easily altered at the level of the nearest neighbors, through local vibrations and thermal expansion, without rearranging molecules over long distances. As a structure indicator, enthalpy is more sensitive to the nearest neighbors than to the longer-range structure and this is perhaps why we find enthalpy in the same group with intermolecular spacings in its response to cooling rate.

It is intriguing that the two timescales for kinetic arrest correspond to the two relaxation modes observed by DS. The interpretation of these relaxation modes as fast rotation about the long axis (α) and slow rotation end-over-end (δ) is consistent with the picture proposed above. Between the two processes, the δ mode has a larger activation volume in the sense that molecules in the log jam must be shoved around for an end-over-end rotation, whereas the α mode requires less coordination with the neighbors and should have a smaller activation volume. It makes sense that

the state of the log jam is frozen at a higher temperature than the axial rotation of the logs. This interpretation is consistent with the literature on glass aging, which indicates that volume relaxation correlate with the α process.[28] In the case of ITZ, TMDSC shows that enthalpy relaxation correlates with α mode.[8]

CONCLUSIONS

In this study, we characterized structural features in both smectic and lateral packing in ITZ liquids and glasses prepared by different cooling rates through synchrotron scattering and local X-ray scattering, and determined the cooling rate effects on structural features frozen in glasses for the first time. We find these glasses have very different glass structures, with faster cooling leading to lower smectic order, less regular lateral packing, and larger inter- and intralayer spacing. These different structures can be characterized by two fictive temperatures, the higher one related to the smectic and lateral-packing order and the lower one to molecular spacings and enthalpy. The difference between the two fictive temperatures is as large as 20 K. Our results indicate that the interlayer and intralayer order in a smectic structure rise and fall together as part of liquid crystallinity, whereas the structural features associated with the nearest-neighbor structure can actively evolve when the LC framework is frozen. At each cooling rate, the two fictive temperatures correspond to the glass transition temperatures for the two relaxation modes of ITZ observed by DS. The slower δ mode (end-over-end rotation) corresponds to the freezing of smectic and lateral-packing order. The faster α mode (axial rotation) corresponds to the freezing of smectic and lateral-packing order.

Our results indicate that the different aspects of glass structure can be manipulated independently. This is an ability intrinsic to glass formation when multiple relaxation modes exist. For these systems, multiple kinetic arrests can be engineered to target selected structural features. Apart from the anisotropy of molecular shape, multiple relaxation modes can arise from the presence of slow and fast components in a mixture. Application of this principle could lead to glasses with tailor-made properties for applications in organic electronics and pharmaceutics. Future progress in this area will benefit from the determination of the range over which the fictive temperatures can differ in the same glass and how the fictive temperatures evolve during glass aging. Since two timescales are involved in glass preparation, it is of interest to determine whether the same two timescales control glass aging.

ACKNOWLEDGEMENTS

We thank NSF for supporting this work and the NSF-supported University of Wisconsin Materials Research Science and Engineering Center (DMR-1720415) for the use of its characterization facility.

REFERENCES

(1) Gujral, A.; Yu, L.; Ediger, M. Anisotropic organic glasses. *Current Opinion in Solid State and Materials Science* **2018**, *22* (2), 49-57.
(2) Bagchi, K.; Ediger, M. D. Controlling structure and properties of vapor-deposited glasses of organic semiconductors: Recent advances and challenges. *The Journal of Physical Chemistry Letters* **2020**, *11* (17), 6935-6945.
(3) Teerakapibal, R.; Huang, C.; Gujral, A.; Ediger, M. D.; Yu, L. Organic glasses with tunable liquid-crystalline order. *Physical review letters* **2018**, *120* (5), 055502.
(4) Chen, Z.; Yu, J.; Teerakapibal, R.; Meerpoel, L.; Richert, R.; Yu, L. Organic glasses with tunable liquid-crystalline order through kinetic arrest of end-over-end rotation: the case of saperconazole. *Soft Matter* **2020**, *16* (8), 2025-2030.
(5) Chen, Z.; Bishop, C.; Thoms, E.; Bock, H.; Ediger, M. D.; Richert, R.; Yu, L. Controlling the Columnar Order in a Discotic Liquid Crystal by Kinetic Arrest of Disc Tumbling. *Chemistry of Materials* **2021**, *33* (12), 4757-4764.
(6) Yokoyama, D. Molecular orientation in small-molecule organic light-emitting diodes. *Journal of Materials Chemistry* **2011**, *21* (48), 19187-19202.
(7) Yang, D.-K.; Wu, S.-T. *Fundamentals of liquid crystal devices*; John Wiley & Sons, 2014.
(8) Tarnacka, M.; Adrjanowicz, K.; Kaminska, E.; Kaminski, K.; Grzybowska, K.; Kolodziejczyk, K.; Wlodarczyk, P.; Hawelek, L.; Garbacz, G.; Kocot, A. Molecular dynamics of itraconazole at ambient and high pressure. *Physical Chemistry Chemical Physics* **2013**, *15* (47), 20742-20752.
(9) Brás, A.; Dionísio, M.; Huth, H.; Schick, C.; Schönhals, A. Origin of glassy dynamics in a liquid crystal studied by broadband dielectric and specific heat spectroscopy. *Physical Review E* **2007**, *75* (6), 061708.
Kremer, F.; Schönhals, A. *Broadband dielectric spectroscopy*; Springer Science & Business Media, 2002.
Martin, A. J.; Meier, G.; Saupe, A. Extended Debye theory for dielectric relaxations in nematic liquid crystals. In *Symposia of the Faraday Society*, 1971; Royal Society of Chemistry: Vol. 5, pp 119-133.
(10) Schönhals, A.; Zubowa, H. L.; Fricke, R.; Frunza, S.; Frunza, L.; Moldovan, R. On the Dielectric Behavior of Unaligned Samples of 4-n-Octyl-4′-cyanobiphenyl (8CB). *Crystal Research and Technology: Journal of Experimental and Industrial Crystallography* **1999**, *34* (10), 1309-1314.
(11) Kaafarani, B. R. Discotic liquid crystals for opto-electronic applications. *Chemistry of Materials* **2011**, *23* (3), 378-396.
(12) Benmore, C.; Mou, Q.; Benmore, K.; Robinson, D.; Neuefeind, J.; Ilavsky, J.; Byrn, S.; Yarger, J. A SAXS-WAXS study of the endothermic transitions in amorphous or supercooled liquid itraconazole. *Thermochimica Acta* **2016**, *644*, 1-5.
(13) Hammersley, A. FIT2D: a multi-purpose data reduction, analysis and visualization program. *Journal of Applied Crystallography* **2016**, *49* (2), 646-652.
(14) Benmore, C. J. X-Ray Diffraction from Glass. *Modern Glass Characterization* **2015**, 1-30.
(15) Heiney, P. A. Datasqueeze: A software tool for powder and small-angle X-ray diffraction analysis. *Newsletter of the IUCr Commission on Powder Diffraction* **2005**, *32*, 9-11.
(16) McMillan, W. X-ray scattering from liquid crystals. I. Cholesteryl nonanoate and myristate. *Physical Review A* **1972**, *6* (3), 936.
(17) Takanishi, Y.; Ikeda, A.; Takezoe, H.; Fukuda, A. Higher smectic-layer order parameters in liquid crystals determined by x-ray diffraction and the effect of antiferroelectricity. *Physical Review E* **1995**, *51* (1), 400.
(18) Greet, R.; Turnbull, D. Glass transition in o-terphenyl. *The Journal of Chemical Physics* **1967**, *46* (4), 1243-1251.
(19) Madhusudana, N.; Srikanta, B.; Subramanya Raj Urs, M. Studies on some smectogenic compounds with large bilayer spacings. *Molecular Crystals and Liquid Crystals* **1983**, *97* (1), 49-75.

(20) Kapernaum, N.; Giesselmann, F. Simple experimental assessment of smectic translational order parameters. *Physical Review E* **2008**, *78* (6), 062701.
(21) Jones, A.; Misell, D. A practical method for the deconvolution of experimental curves. *British Journal of Applied Physics* **1967**, *18* (10), 1479.
(22) Perry, P. t.; Throop, G. Decay of pair correlations in hard sphere fluids. *The Journal of Chemical Physics* **1972**, *57* (5), 1827-1829.
(23) Moynihan, C.; Lee, S.-K.; Tatsumisago, M.; Minami, T. Estimation of activation energies for structural relaxation and viscous flow from DTA and DSC experiments. *Thermochimica acta* **1996**, *280*, 153-162.
(24) Hensel, A.; Schick, C. Relation between freezing-in due to linear cooling and the dynamic glass transition temperature by temperature-modulated DSC. *Journal of non-crystalline solids* **1998**, *235*, 510-516.
(25) Clough, S.; Blumstein, A.; Hsu, E. Structure and thermal expansion of some polymers with mesomorphic ordering. *Macromolecules* **1976**, *9* (1), 123-127.
(26) Leadbetter, A.; Frost, J.; Gaughan, J.; Gray, G.; Mosley, A. The structure of smectic A phases of compounds with cyano end groups. *Journal de Physique* **1979**, *40* (4), 375-380.
(27) Palermo, M. F.; Pizzirusso, A.; Muccioli, L.; Zannoni, C. An atomistic description of the nematic and smectic phases of 4-n-octyl-4′ cyanobiphenyl (8CB). *The Journal of chemical physics* **2013**, *138* (20), 204901.
(28) Simon, S.; Sobieski, J.; Plazek, D. Volume and enthalpy recovery of polystyrene. *Polymer* **2001**, *42* (6), 2555-2567.